Spectrophotometric and Steady-State Kinetic Analysis of the Biosynthetic Arginine Decarboxylase of *Yersinia pestis* Utilizing Arginine Analogues as Inhibitors and Alternative Substrates†

Paul B. Balbo, Chandra N. Patel, Korie G. Sell, Robert S. Adcock, Sundar Neelakantan, Peter A. Crooks, and Marcos A. Oliveira*

College of Pharmacy, Center for Structural Biology, and Markey Cancer Center, University of Kentucky, Lexington, Kentucky 40536

Received March 17, 2003; Revised Manuscript Received September 30, 2003

ABSTRACT: The PLP-dependent, biosynthetic arginine decarboxylase (ADC) of *Yersinia pestis* was investigated using steady-state kinetics employing structural analogues of arginine as both alternative substrates and competitive inhibitors. The inhibitor analysis indicates that binding of the carboxyl and guanidinium groups of the substrate, L-arginine, provides essentially all of the free energy change realized upon substrate binding in the ground state. Furthermore, recognition of the guanidinium group is primarily responsible for substrate specificity. Comparison of the steady-state parameters for a series of alternative substrates that contained chemically modified guanidinium moieties provides evidence of a role for induced fit in ADC catalysis. ADC was also characterized by UV/vis and fluorescence spectrophotometry in the presence or absence of a number of arginine analogues. The enzyme complexes formed served as models for the adsorption complex and the external aldimine complex of the enzyme with the substrate.

The amino acids L-arginine and L-ornithine are both precursors in the synthesis of putrescine (1,4-diaminobutane), the first polyamine formed in the general polyamine biosynthesis pathway of most organisms (*1*). Both precursors are enzymatically decarboxylated to yield an amine product. The PLP-dependent enzyme, biosynthetic arginine decarboxylase (ADC),[1] represents the entry point for L-arginine in this pathway (*2*) and catalyzes the irreversible decarboxylation of L-arginine to form agmatine (1-amino-4-guanidinylbutane) and CO_2.

PLP-dependent enzymes are capable of catalyzing a variety of chemical reactions including racemization, transamination, retro-aldol cleavage, and decarboxylation (*3*−*5*). Scheme 1 illustrates the basic mechanism for ADC catalysis consistent with the general mechanism for PLP-dependent, enzymatic amino acid decarboxylation. The free enzyme, **E**, is depicted at the top of Scheme 1 and is characterized by having a PLP cofactor covalently attached via the formation of a Schiff base (internal aldimine) to the ϵ-amino group of a catalytic Lys residue located at the active site. In Scheme 1, proceeding left from **E**, the enzyme combines with the substrate, L-arginine, to form the adsorption complex (Michaelis complex, E·S), depicted as intermediate **I**. After formation of the adsorption complex, the imine carbon of the internal

Scheme 1: General Catalytic Mechanism for ADC

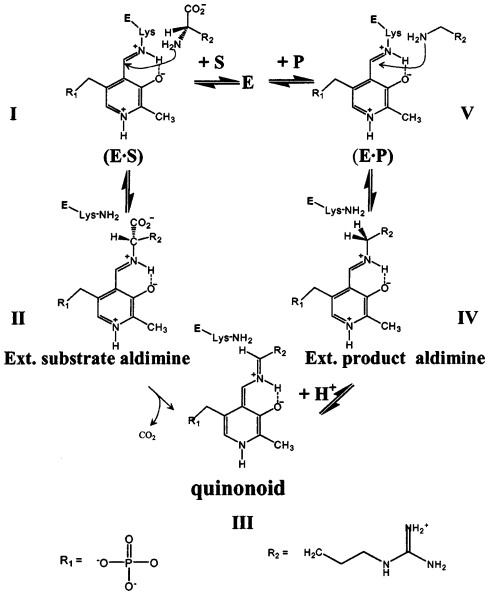

aldimine is subject to nucleophilic attack by the α-amino group of the substrate. This results in the formation of the Schiff base between cofactor and substrate, referred to as the external substrate aldimine (Scheme 1, intermediate **II**). The irreversible decarboxylation of **II** yields the quinonoid intermediate, **III**. Catalysis requires the rotation about the bond between the imine nitrogen and the C_α of the amino acid to orient the carboxyl group such that the labile $C-COO^-$ σ-bond orbital becomes nearly perpendicular to the plane of the pyridine ring system of the cofactor (*4*). Stabilization of this conformation is most likely controlled

† Supported by American Association of Colleges of Pharmacy (AACP), an NIP award, and in part by the Kentucky Lung Cancer Research Program (KLCR).

* To whom correspondence should be addressed. Phone: (859) 323-2710. Fax: (859) 257-7585. E-mail: moliv2@email.uky.edu.

[1] Abbreviations: ADC, biosynthetic arginine decarboxylase; PLP, pyridoxal-5′-phosphate; ODC, ornithine decarboxylase; ALR, alanine racemase; DapDC, diaminopimelate decarboxylase; PEPC, phosphoenolpyruvate carboxylase; MDH, malate dehydrogenase.

10.1021/bi0344127 CCC: $25.00
Published on Web 12/05/2003

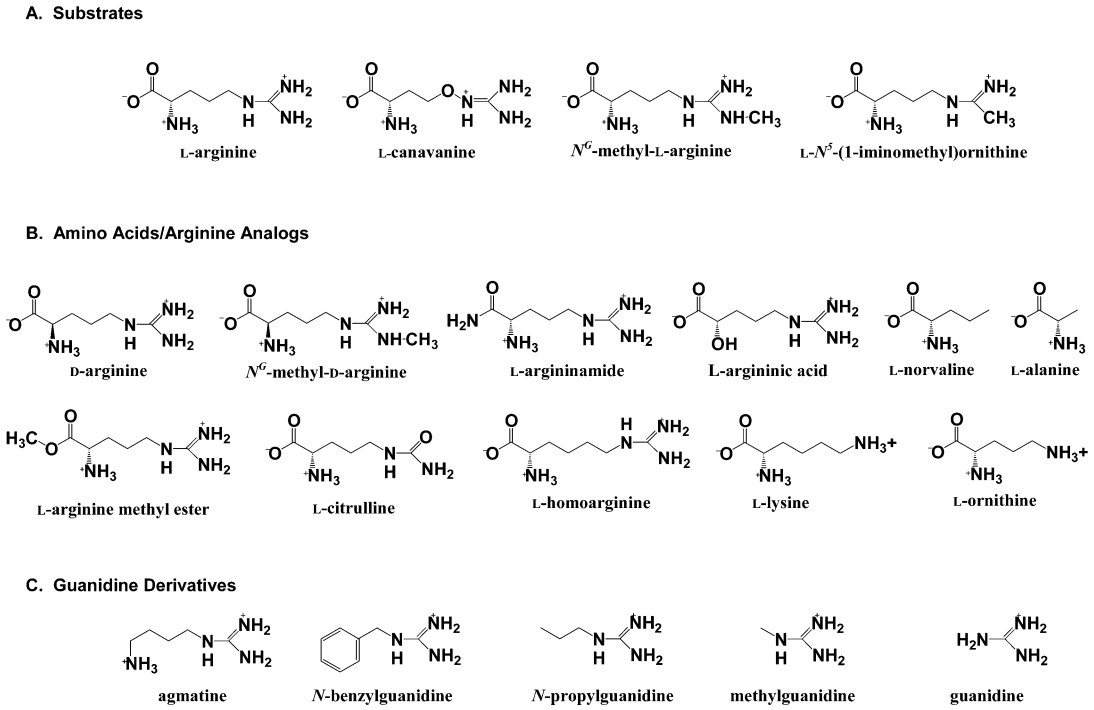

FIGURE 1: Arginine structural analogues and guanidine derivatives used in this study.

by interactions between functional groups of the substrate (possibly carboxyl and/or guanidinium groups) and active site residues. Furthermore, the pyridine ring is highly electron-withdrawing, which promotes the delocalization of electrons during catalysis into the azaaromatic ring system (*6*). Protonation of **III** at the C_α results in the formation of intermediate **IV**, which is the external aldimine of PLP and the amine product, agmatine. Nucleophilic attack by the catalytic Lys residue regenerates the internal aldimine, forming the adsorption complex between enzyme and product (**E**·**P**, intermediate **V**). Dissociation of the product regenerates **E** and completes the catalytic cycle.

In the present study, a steady-state kinetic analysis of recombinant ADC from *Y. pestis* was performed employing structural analogues of L-arginine as inhibitors and alternative substrates. The list of analogues used in this study as substrates and inhibitors and their chemical structures is given in Figure 1. UV/vis and fluorescence spectrophotometric analysis of ADC was also conducted in the presence or absence of certain arginine analogues, which were selected to serve as model compounds in the characterization of the adsorption complex (L-argininic acid) and the external aldimine complex with substrate (L-argininamide and L-arginine methyl ester). Evidence is also presented for the role of induced fit in ADC catalysis.

MATERIALS AND METHODS

Cloning and Protein Purification. The *Yersinia pestis* ADC gene (1980 bp) was cloned from genomic DNA in two roughly 1 kb fragments connected by an internal BstEII site at position 1094, using the following primers (restriction endonuclease sites underlined): N-terminal fragment, forward primer: 5′-TCCGAATTCGATGTCTGATGATAACT-TGATTAGCCGTCCG-3′; N-terminal fragment, reverse primer: 5′-GTGAGCGGTAACCGCACGACC-3′; C-terminal fragment, forward primer: 5′-CTGGTCGTGCGGTTACC-GC-3′; and C-terminal fragment, reverse primer: 5′-TAA-CTCGAGTTCGTCTTCAAGATATGTGTAGCCG-3′. The N- and C-terminal cloned fragments contained restriction sites for EcoRI/BstEII and BstEII/XhoI, respectively. A Boehringer Mannheim Expand Long Template PCR System was used for the PCR. The TA cloning kit containing the pCR 2.1 vector (Invitrogen) was subsequently used to clone the PCR products. The fragments were then cloned together into the EcoRI and Xho I restriction sites in the pET-28b vector (Novagen), which incorporates a six-residue, C-terminal His tag. The cloned pET-28b vector containing the recombinant ADC gene was transformed into BL21(DE3)-pLysE (Invitrogen) competent *Escherichia coli* cells.

Transformed *E. coli* cells were grown to an OD of 0.5−0.8 and then induced with a final concentration of 1 mM IPTG. The cells were then allowed to grow at room temperature for 6 h and harvested by centrifugation. The cell pellet was resuspended in lysis buffer (20 mM Tris pH 8.5, 10 mM $MgCl_2$ containing lysozyme (Sigma)) at 15 mg/L cell culture. The resuspended cells were then disrupted by sonication and clarified by centrifugation (8000 rpm in a Beckman Type 45 Ti rotor for 20 min). The clarified supernatant was passed over a Ni-NTA agarose (Qiagen) column. The buffer used during chromatography was 30 mM Tris pH 8.5, containing 10 mM $MgCl_2$ and 40 μM PLP. After the sample was applied, the column was washed first with 5 column volumes of buffer, followed by 5 column volumes of buffer containing 30 mM imidazole; the protein was then eluted in buffer containing 90 mM imidazole. Column fractions containing ADC were pooled, concentrated, and exchanged into 0.1 M HEPES pH 7.5, containing 5 mM $MgCl_2$ and 10 μM PLP by ultrafiltration using a Centricon30 device (Millipore). Protein concentration was determined by measuring absorbance at 280 nm (A_{280}) after determining the mass extinction coefficient at this wavelength ($\epsilon^{0.1\%}_{280}$).

First, the ADC concentration was determined by the BCA method (*7*) against a bovine serum albumin (BSA) standard, which was determined using its published mass extinction coefficient. From the BCA-determined value, the mass extinction coefficient at 280 nm ($\epsilon^{0.1\%}_{280}$) for *Y. pestis* ADC was calculated from an average of three determinations and found to be 0.87 ± 0.01 L g^{-1} cm^{-1}. The purity of all protein preparations was determined using SDS−PAGE and isoelectric focusing (IEF) (data not shown).

Arginine Analogues and General Reagents. All buffers and chemicals used were of analytical quality. The following compounds were purchased from Sigma-Aldrich: L-arginine·HCl, D-arginine·HCl, N^G-methyl-L-arginine·HCl, N^G-methyl-D-arginine·HCl, L-arginine methyl ester·2HCl, L-canavanine·H_2SO_4, L-N^5-(1-iminoethyl)ornithine·HCl, L-argininamide·2HCl, L-homoarginine·HCl, agmatine·H_2SO_4, methylguanidine·HCl, guanidine·HCl, L-lysine·HCl, L-ornithine·HCl, D-ornithine·HCl, L-citrulline, and L-norvaline·HCl. L-Argininic acid was purchased from Research Organics (Cleveland, OH). The enzymes phosphoenolpyruvate carboxylase (PEPC) and malate dehydrogenase (MDH) were purchased as lyophilized powders from CalBiochem (La Jolla, CA). PEPC and MDH stock solutions were prepared in 50 mM Tris·HCl, pH 7.5, containing 5 mM $MgCl_2$, 30% glycerol and stored as frozen aliquots at −80 °C. Prior to undertaking the kinetic analysis of ADC, the specific activities of both PEPC and MDH, as prepared here, under the conditions of the ADC kinetic assay (described next), were determined to be 10.2 and 2375 U/mg protein, respectively, where one U is equal to 1 μmol of product formed per min.

Synthesis of N-Substituted Guanidines. The compounds *N*-benzylguanidine and *N*-propylguanidine were synthesized according to the following procedure, which was adapted from ref *8*. To either benzylamine (0.005 mol, 535 mg) or propylamine (0.005 mol, 295 mg) was added 10 mL of 30% ammonium hydroxide, followed by *S*-ethylisothiourea hemisulfate salt (700 mg, 0.005 mol) in a 50 mL round-bottomed flask. The mixture was heated to 70 °C and stirred vigorously until the reactants dissolved. There was a vigorous evolution of ethyl mercaptan. The mixture was stirred at 70 °C until no effervescence of ethylmercaptan was detected (~6 h). The mixture was then cooled to room temperature and evaporated to dryness under reduced pressure in a rotary evaporator. The residue obtained was then dissolved in water, and the insoluble, unreacted *S*-ethylisothiourea was filtered off. Concentration of the filtrate to dryness in vacuo afforded a white solid, which was washed with chloroform (20 mL) and dried under vacuum. *N*-Benzylguanidine: (yield: 520 mg, 70%); ^{1}H NMR (300 MHz, D_2O with TSP internal standard): δ 7.40 (5H, m), 4.42 (2H, s) ppm; ^{13}C NMR (75 MHz, D_2O with TSP internal standard): δ 160.2, 142.3, 128.5, 127.3, 126.4, 46.4 ppm; mass Spectrum (Maldi): *m*/*z* 150 MH$^+$. *N*-Propylguanidine: (yield: 710 mg, 78.5%); ^{1}H NMR (300 MHz, D_2O with TPS internal standard): δ 3.35 (2H, t), 2.9 (2H, t), 2.0 (2H, m) ppm; ^{13}C NMR (75 MHz, D_2O with TPS internal standard): δ 159.1, 50.5, 42.2, 26.3 ppm.

ADC Kinetics. The initial rates of decarboxylation of L-arginine or alternate substrates as a function of substrate concentration were measured at 37 °C using a continuous, coupled enzyme assay similar to that described previously (*9*). Briefly, the assay couples the decarboxylation of the amino acid substrate to the carboxylation of phosphoenolpyruvate to form oxaloacetate and phosphate, which in turn is coupled to the NADH-dependent reduction of oxaloacetate to form malate and NAD^+. The rate of product formation was continuously monitored spectrophotometrically using a Cary 50 UV/vis spectrophotometer (Varian Scientific Instruments) and a $\Delta\epsilon_{340}$ of −6.22 mM^{-1} cm^{-1} for the conversion of NADH to NAD^+ at 340 nm. The standard assay (600 μL) included 0.1 M HEPES, pH 7.5 buffer, containing 5 mM $MgCl_2$, 40 μM pyridoxal phosphate, 170 μM NADH, 2.5 mM phosphoenol pyruvate, 2.75 U phosphoenol pyruvate carboxylase (PEPC), 0.51 U malate dehydrogenase (MDH), a variable amount of substrate, and an appropriate amount of ADC (10−0.1 μg). An identical assay was employed in the measurement of initial rates of L-arginine decarboxylation in the presence of various inhibitors, except that the initial concentration of L-arginine was 313 μM, and the concentration of each inhibitor was varied around its K_i.

Spectrophotometric Measurements of ADC. ADC samples for spectrophotometric analysis were subject to ultrafiltration to remove excess pyridoxal phosphate. This procedure consistently produced a protein with a constant A_{280}/A_{420} ratio and resulted in no loss of specific activity, indicating that the PLP cofactor remained bound. Absorption spectra of ADC were measured at 37 °C using a Cary 50 UV/vis spectrophotometer (Varian Scientific Instruments). Experimental conditions were 0.1 M HEPES, pH 7.5 buffer, containing 5 mM $MgCl_2$ and 0.98 mg/mL ADC. In measuring UV/vis absorption spectra as a function of pH, the conditions remained the same except that buffer contained 0.1 M each MES, HEPES, and CHAPS; the pH was adjusted with NaOH. Fluorescence excitation and emission spectra were measured at 25 °C using a Shimadzu RF-5301 PC fluorescence spectrometer. Experimental conditions were 0.1 M HEPES, pH 7.5 buffer, containing 5 mM $MgCl_2$ and 0.084 mg/mL ADC. The instrument response time was set to 0.1 s, and the slit width was set to either 5 or 10 nm.

Data Analysis. All kinetic and binding data were subject to nonlinear regression analysis using SigmaPlot 2000. A simplified Michaelis−Menten description (eq 1a) for a single-substrate enzyme was used to model the steady-state kinetics of ADC. Steady-state kinetics data for the decarboxylation of L-arginine or alternative substrates were analyzed according to the Michaelis−Menten equation, eq 1b.

$$\mathrm{E} + \mathrm{S} \underset{k_{-1}}{\overset{k_1}{\rightleftharpoons}} \mathrm{ES} \xrightarrow{k_{cat}} \mathrm{E} + \mathrm{P} \tag{1a}$$

$$v = \frac{V_{max}[\mathrm{S}]}{K_m + [\mathrm{S}]} \tag{1b}$$

Steady-state kinetics data for ADC in the presence of inhibitors were analyzed according to the reversible, dead-end (competitive) inhibition model, described in eq 2.

$$v = \frac{V_{max}}{1 + \frac{K_m}{[\mathrm{S}]}\left(1 + \frac{[\mathrm{I}]}{K_i}\right)} \tag{2}$$

In both cases, v is the measured initial velocity with units

Table 1: Steady-State Kinetic Parameters for Arginine Decarboxylase

substrate	k_{cat} (s^{-1})	K_m (mM)	k_{cat}/K_m (M^{-1} s^{-1})
L-arginine	5.46 ± 0.32	0.200 ± 0.037	2.73×10^4
N^G-methyl-L-arginine	1.22 ± 0.13	0.163 ± 0.044	7.51×10^3
L-canavanine	0.111 ± 0.005	0.233 ± 0.049	4.67×10^2
L-N^5-(iminoethyl)-ornithine	0.419 ± 0.038	9.53 ± 1.61	4.40×10^1

of μmol/min mg ADC; V_{max} is the maximum velocity; K_m is the apparent Michaelis constant for the substrate; K_i is the apparent inhibition constant; and [S] and [I] are the molar concentrations of the substrate and inhibitor, respectively. A value of 70 kDa for the molecular weight of an ADC monomer (*10*), and the equivalent of one active site per monomer, was used in the calculation of k_{cat}.

The apparent equilibrium dissociation constants (K_d) for the inhibitors L-argininamide and L-arginine methylester were determined from the UV/vis absorption differences observed as a function of inhibitor concentration, [I], according to eq 3.

$$(A_{max} - A) = \frac{(A_{max} - A_{min})[I]}{[I] + K_d} \quad (3)$$

A is the absorbance at 410 nm, corresponding to the difference absorbance maximum observed upon ligand association, and A_{max} and A_{min} are the maximum and minimum values at 410 nm, respectively. The term ($A_{max} - A_{min}$) was determined by best-fit of the data, as was K_d. The absorbance data are reported next as the fraction of binding sites bound by inhibitor, termed fraction saturated, calculated by $[(A_{max} - A)/(A_{max} - A_{min})]$.

RESULTS

Steady-State Kinetic Analysis of ADC. The steady-state kinetic parameters for ADC (at 37 °C, pH 7.5) utilizing either the natural substrate, L-arginine, or the alternative substrates, N^G-methyl-L-arginine, L-canavanine, or L-N^5-(1-iminoethyl)-ornithine, were determined; the results are given in Table 1. It is evident that the high K_m value (9.5 mM) for L-N^5-(iminoethyl)ornithine is due to poorer binding of the acetamidinium group relative to that of the guanidinium group of L-arginine. Additionally, the following amino acids were tested for their suitability as substrates and showed no activity at concentrations as high as 20 mM: D-arginine, N^G-methyl-D-arginine, L-homoarginine, L-citrulline, L-norvaline, L-alanine, L-ornithine, D-ornithine, L-lysine, and D-lysine. To investigate the determinants for substrate recognition by ADC, a steady-state kinetic analysis was conducted with a series of inhibitors that are arginine structural analogues and include amino acids, amino acid derivatives, and guanidine derivatives. These results are listed in Table 2. Additionally, the following compounds were tested and showed no apparent inhibition at concentrations as high as 10 mM: L-lysine, L-ornithine, D-ornithine, L-citrulline, L-norvaline, and L-alanine.

Spectrophotometric Analysis of ADC. To characterize the nature of ADC alone and in complex with product and inhibitors, UV/vis and fluorescence spectroscopy was employed. UV/vis and fluorescence spectroscopy can be used to probe the tautomeric and ionic states of the PLP cofactor (*11*−*15*). PLP structures relevant to this work are shown in Figure 2. The tautomeric ketoenamine and enolimine species are protonated at either the imine-N or phenolic-O atoms, respectively. Model studies have established that the ketoenamine form predominates in a polar environment, whereas the enolimine form predominates in an apolar environment (*16*).

Table 2: Inhibition Constants for Arginine Decarboxylase Inhibitors

inhibitor	K_i[a] (mM)	ΔG[b] (kcal/mol)	$\Delta\Delta G$[c] (kcal/mol)
arginine analogues			
D-arginine	0.0206 ± 0.0022	−6.64	−1.39
N^G-methyl-D-arginine	0.168 ± 0.027	−5.35	−0.10
L-arginine methyl ester	0.189 ± 0.017	−5.28	−0.03
L-argininic acid	0.327 ± 0.075	−4.94	+0.31
L-canavanine	0.427 ± 0.042	−4.77	+0.48
L-argininamide	0.897 ± 0.074	−4.32	+0.93
L-homo-arginine	1.53 ± 0.15	−3.99	+1.26
guanidine derivatives			
N-benzylguanidine	1.40 ± 0.08	−4.05	+1.20
N-propylguanidine	1.93 ± 0.36	−3.85	+1.40
agmatine	2.77 ± 0.24	−3.63	+1.62
methylguanidine	3.09 ± 0.03	−3.56	+1.69
guanidine	3.39 ± 0.37	−3.50	+1.75

[a] Reported errors are the standard errors determined during nonlinear regression analysis. [b] The observed free energy change upon inhibitor binding; $\Delta G = -RT \ln(K)$, where $K = 1/K_i$ in M^{-1}. [c] The observed difference in free energy change upon inhibitor binding relative to that of the substrate, L-arginine, of −5.25 kcal/mol (estimated using K_m = 200 μM, determined in this work). $\Delta\Delta G = \Delta G_{inhibitor} - \Delta G_{L-Arg}$.

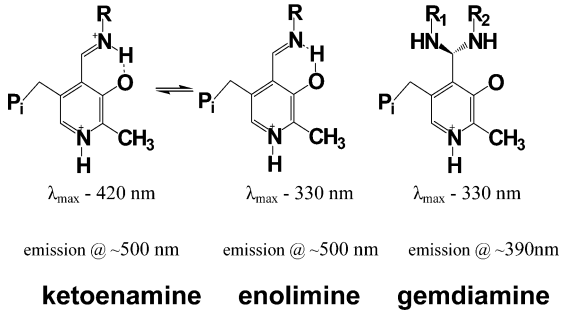

FIGURE 2: Spectroscopic properties of PLP adducts. The absorbance maximum (λ_{max}) as well as the fluorescence emission (EM) wavelength, corresponding to excitation at the absorption wavelength for each species, is shown below the corresponding structure, where applicable. Although not depicted in the figure, the deprotonated form of the ketoenamine has a characteristic absorbance maximum at 350 nm.

The UV/vis spectra of ADC in the presence or absence of various inhibitors are shown in Figure 3. Native ADC (Figure 3, spectrum A) has an absorption peak at 417 nm, which can be assigned to the internal aldimine form of the PLP cofactor. The prominence of the 417 nm peak and the absence of significant features at 330 nm indicate that the PLP cofactor is predominantly in the (protonated) ketoenamine tautomeric form rather than the enolamine form (*15*). In the presence of either L-argininamide or L-arginine methyl ester (Figure 3, spectra B and C, respectively), the 417 nm peak exhibits a red-shift to about 422 nm and exhibits a slight decrease in intensity. This is consistent with the formation of an external aldimine. The minor 350 nm peak exhibited in these spectra increases with the concomitant

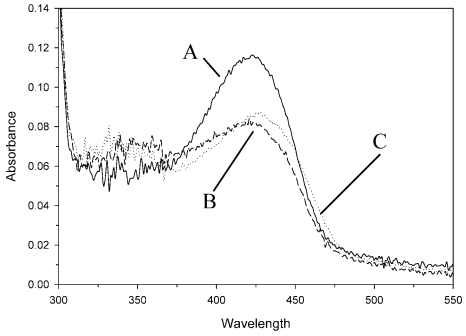

FIGURE 3: UV/vis absorbance spectroscopy of ADC. UV/vis spectra of ADC are shown in the absence or presence of various ligands: (A) native ADC, (B) ADC + 7.4 mM L-argininamide, (C) ADC + 2.4 mM L-arginine methyl ester, and (D) ADC + 11.5 mM agmatine. The sample conditions are 1.0 mg/mL ADC, 0.1 M HEPES, pH 7.5, and 5 mM $MgCl_2$ in all cases.

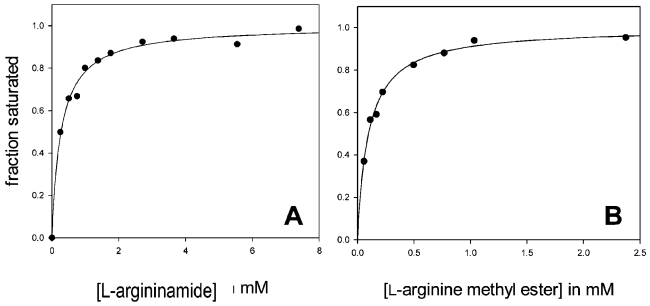

FIGURE 4: Determination of K_d for selected enzyme−inhibitor complexes. Inhibitor saturation binding curves for ADC at 37 °C as a function of the concentration of the substrate analogues (A) L-argininamide and (B) L-arginine methyl ester as monitored by the absorbance change at 410 nm. Sample conditions in all cases were 1.0 mg/mL ADC, 0.1 M HEPES, pH 7.5, and 5 mM $MgCl_2$. The lines represent the best-fit of the data; the K_d values determined from this analysis were 276 ± 26 μM, for L-argininamide, 98 ± 7 μM and for L-arginine methyl ester, and 8.1 ± 1.3 mM for agmatine.

decrease of the 420 nm peak when the pH is made more alkaline (data not shown), indicating that the 350 nm peak corresponds to the deprotonated ketoenamine form of the cofactor. In contrast, the UV/vis spectrum of native ADC is invariant in the pH range 6.5−9.0. Additionally, the ADC spectrum remained essentially unchanged from that of the native ADC upon the addition of L-argininic acid (see Figure 3, curve A for comparison), which suggests that the ionic and tautomeric states of the PLP cofactor remain essentially unchanged upon formation of the adsorption complex. Furthermore, the ADC spectrum in the presence of D-arginine exhibited a change consistent with the formation of an external aldimine; however, this is most likely an artifact since the absorbance change was incomplete at D-arginine concentrations 100-fold greater than its K_i (data not shown). This indicates that the strong inhibition observed for this compound (K_i = 21 μM) occurs via formation of the adsorption complex. The fluorescence emission spectrum from 350 to 600 nm (excitation at 390 nm) was essentially the same for the enzyme complexed with either D-arginine, L-argininamide, L-arginine methylester, or uncomplexed (data not shown).

The spectroscopic characterization of ADC in complex with agmatine was attempted. It was discovered that this resulted in the formation of a PLP−agmatine adduct that could be mostly separated from the protein by ultrafiltration. After subtraction of the spectrum of the filtrate from the combined spectrum, it was qualitatively determined that the remaining agmatine−enzyme complex exhibited an absorption maximum at 420 nm, consistent with the formation of an external aldamine (data not shown).

The characteristic absorbance changes upon the formation of the external aldimine containing the substrate analogues (L-argininamide and L-arginine methyl ester) allowed for the determination of apparent equilibrium dissociation constants (K_d) for these compounds. Data from these experiments are shown in Figure 4; results are provided in the figure caption.

DISCUSSION

Prokaryotic, biosynthetic ADC (*E. coli*) was first isolated and characterized by Wu and Morris (*10*, *17*). *Y. pestis* ADC is 37% identical to the *E. coli* enzyme at the amino acid level. Our determination of k_{cat} of 5.46 s^{-1} at pH 7.5 agrees very well with the earlier data (Figure 6 in ref *10*), supporting the notion that the two bacterial enzymes are very similar. The steady-state kinetic model employed here is the simplified Michaelis−Menten description of an enzyme having one substrate (eq 1a), and the ratio, k_{-1}/k_1, is an apparent dissociation constant (K_d) for ES; analogously, K_i is an apparent dissociation constant for the enzyme−inhibitor complex, EI. For the ADC mechanism, the K_d constant incorporates a term for the formation of the adsorption complex and another for the external aldimine (intermediates **I** and **II**, respectively, Scheme 1). Furthermore, the k_{cat} term comprises several steps, including the irreversible decarboxylation step and the product release step(s). When k_{cat} is small relative to k_{-1}, K_m will closely approximate the apparent K_d or K_i for the substrate or substrate analogue, respectively. Because inhibitors such as L-canavanine and L-argininic acid are chemically very similar to L-arginine, the K_i for these inhibitors are good approximations for K_d of the substrate L-arginine. Furthermore, the data (Tables 1 and 2) show that substrate binding in the ground state is generally not sensitive to desamino and modest N^G-alkyl modifications of the substrate.

Structural and Mechanistic Comparison of ADC with ODC and Other Fold III PLP Enzymes. Biosynthetic ADC is a member of the fold III PLP-dependent class of enzymes, which also includes alanine racemase (ALR), diaminopimelate decarboxylase (DapDC), and mammalian/protoazoan ornithine decarboxylase (ODC). X-ray crystal structures for the ALR (*18*, *19*), DapDC (*20*, *21*), and ODC (*22*−*24*) representatives of this enzyme class have been reported. The fold III PLP-dependent class of enzymes characteristically contains a $(\beta/\alpha)_8$-TIM barrel domain and a β-sandwich domain. These enzymes form dimers via a head-to-tail interaction in which the active site is formed at the interface between the TIM barrel domain of one subunit and the β-sandwich of the other subunit (*18*). The $(\beta/\alpha)_8$-TIM barrel domain contains the conserved, functional motif: [KCN⋯FHVGS⋯GGG⋯ESGR] (*24*, *25*), which contains elements necessary for PLP binding (*26*−*28*), while the β-sandwich domain contains functional groups required for substrate recognition and catalysis (*22*, *29*). A select sequence alignment of ADC (Figure 5) with other fold III PLP enzymes whose structures are known reveals unique structural features

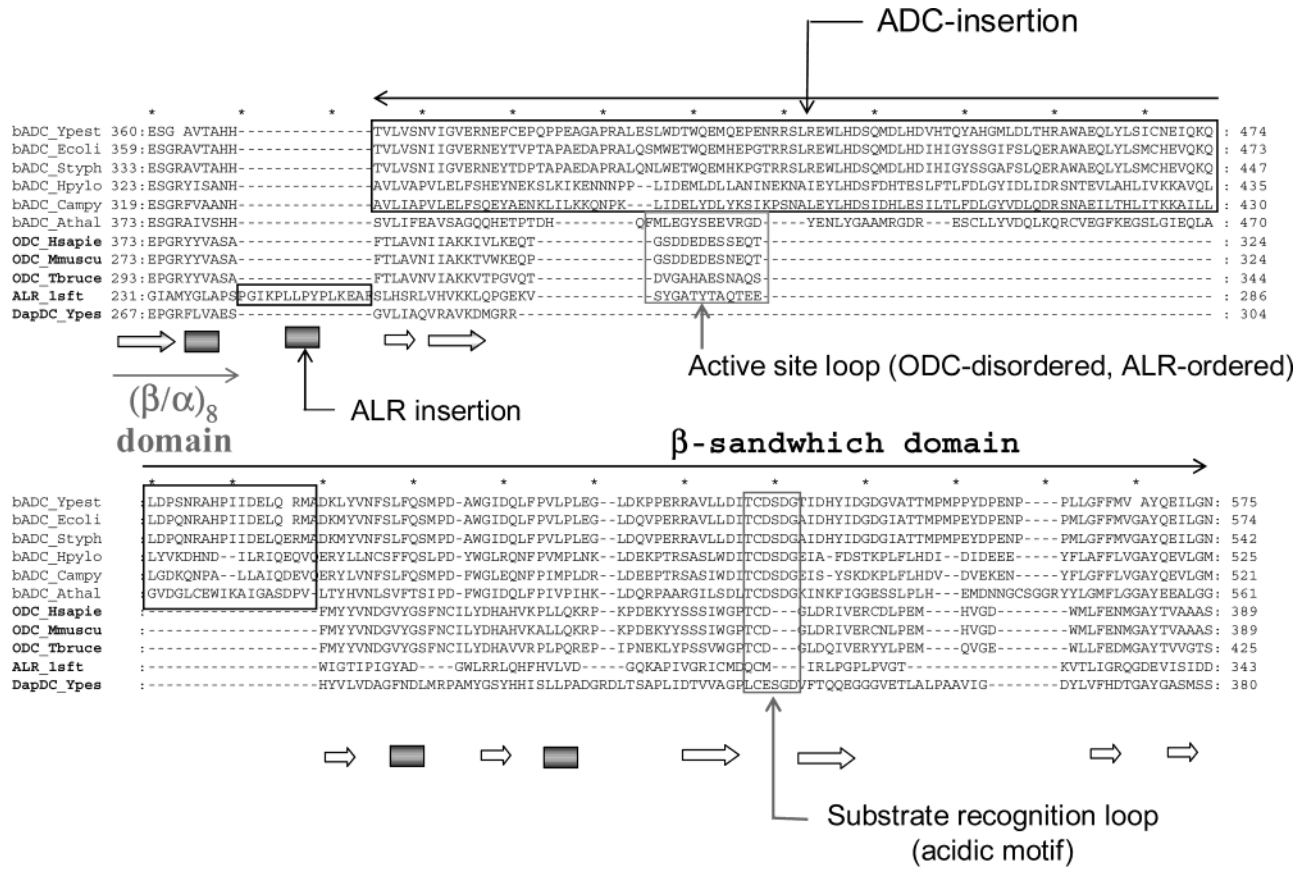

FIGURE 5: Alignment of select ADC sequences and other fold III PLP enzymes. The alignment focuses on the region where ADC has an insertion relative to its other fold III family members. The ADC-insertion maps to the region between the $(\beta/\alpha)_8$ barrel and the β-sandwich domains. The insertion is in a loop that connects two strands of the β-sandwich domain. This loop is an ordered, active site flap in ALR but disordered in the structure of ODC. In ALR, the flap contains a catalytic base, while in ODC this loop has been reported to be involved in enzyme activation by phosphorylation of a serine residue on the loop. A second unique feature of ADC is a substrate recognition loop that, in the structure of ODC, contains an acidic residue involved in the recognition of the δ-amino group of L-ornithine. In ADC, this loop is larger and contains an extra acidic residue that may be a substrate recognition motif for the guanidinium moiety. The secondary structure elements indicated below the sequence alignment in the figure (arrow representing strands, box representing helices) represent those observed in the structures of ODC (PDB code: 1D7K, 1F3T), ALR (1BD0), and DapDC (1HKV (*21*); coordinates for the DapDC structure published by Ray et. al. have not been deposited (*20*)). The sequences shown in the alignment are of ADC from *Y. pestis*, *E. coli*, *S. typhimurium*, *H. pylori*, *C. jejuni*, *A. thaliana*; of ODC from *H. sapiens*, *M. musculus*, *T. brucei*; of ALR from *B. stearothermophilus*; and of DapDC from *Y. pestis*.

of ADC that may have catalytic importance. These features include a substrate recognition loop, a putative active site flap, and a magnesium binding site. In the structure of ODC, the substrate recognition loop contains a conserved aspartic acid that has been shown to interact with the δ-amino group of the product putrescine (*22*). The equivalent region in ADC contains an insertion of three residues with an extra aspartic acid that may be involved in forming the guanidinium recognition pocket (Figure 5). A second unique feature of ADC (Figure 5) is an insertion of ~60 residues relative to its closely related family members (ODC, DapDC, ALR), which maps to a disordered loop in ODC that connects two strands of the β-sandwich domain (*24*). Although this loop is disordered in the structures of ODC, a structurally equivalent loop in the structure of ALR forms an active site flap that contains a catalytic base (*19*), suggesting that ADC may have a large flap domain. Finally, a third unique characteristic of ADC is the requirement for magnesium (*17*), which structurally may be evidence of a link between the enolase superfamily that binds magnesium utilizing a similar $(\alpha/\beta)_8$ TIM barrel fold (*30*, *31*) and fold III PLP enzymes that uses a common phosphate biding motif found in TIM barrels (*32*) to anchor PLP. The latter provides a structural basis for the development of a model for the ADC active site whereby the magnesium and PLP may be next to each other in the ADC active site, with potential implications on tautomeric forms of PLP, its adducts, and its spectroscopic characteristics.

In terms of mechanism, ADC is very similar to mammalian/protozoan ODC (*23*, *33*−*35*). Therefore, a discussion of the important features of the ODC kinetic mechanism is relevant here. The literature values for the steady-state kinetic parameters of ODC are 7.3 ± 0.5 s^{-1} and 320 ± 30 μM for the k_{cat} and K_m for L-ornithine, respectively, at pH 8.0 (*34*, *36*), which are remarkably similar to those of ADC (this paper). Brooks and Phillips undertook an extensive analysis of ODC, employing multiwavelength stopped-flow spectrophotometric analysis at 4 °C to characterize PLP−enzyme intermediates along the reaction coordinate and to determine a minimal kinetic mechanism (*36*). Their results indicated that decarboxylation of the external aldimine of the substrate (equivalent to Scheme 1, intermediate **II**) in the formation of the quinonoid intermediate ($k = 21$ s^{-1}) was not rate-determining. Furthermore, decomposition of the quinonoid intermediate (equivalent to Scheme 1, **III**) was very rapid ($k = 145$ s^{-1}) and followed by at least two steps that were

both rate-determining, including the product release step. These rate-determining steps included: (1) the subsequent conversion of an unidentified intermediate to form the external aldimine of the product, putrescine, and (2) the multistep release of product. Given the close sequence similarity between ADC and ODC, the analogous chemistry catalyzed by each enzyme, and a similar steady-state kinetic behavior, it is reasonable to hypothesize that the two enzymes share key mechanistic features. Furthermore, residues involved in cofactor binding including a key catalytic residue cys360 of ODC, determined by Jackson et al. (*37*), are all strictly conserved in sequence alignments. Although the rate constants for the intermediate steps of ADC catalysis remain to be determined, a rapid chemical step followed by slow product release may be characteristic of ADC.

Determinants of Substrate Recognition by ADC. Analysis of the inhibition constants (K_i) for the series of arginine analogues, including amino acids and guanidine derivatives, identifies the determinants of substrate recognition by ADC. It is clear from a casual inspection of Table 2 that the guanidinium moiety is critically important in substrate binding and specificity. It is also evident that binding of the α-carboxyl group is important. Since the steady-state kinetic data suggest that the K_m for L-arginine (200 μM) is approximately equivalent to its K_d, the observed ΔG for binding L-arginine is estimated to be −5.25 kcal/mol. The observed free energy change of binding for L-argininic acid ($\Delta G = -4.94$ kcal/mol) and L-canavanine ($\Delta G = -4.77$ kcal/mol), substrate analogues that contain both an α-carboxyl and guanidinium group, suggests that binding of the carboxyl and guanidinium groups of the substrate provides essentially all of the free energy change realized upon substrate binding in the ground state.

ADC Kinetics with Alternative Substrates. The inhibitor data clearly indicate that recognition of the guanidinium moiety of the substrate is a major determinant of substrate specificity. However, for the substrates tested here (Table 1), it appears that some degree of substrate specificity of ADC is manifested in the maximal rates of the reaction. Because chemical modification of the guanidinium group would not be expected to exert an inductive effect on the leaving ability of the carboxyl group of the substrate, the differences in k_{cat} among the alternate substrates must be rationalized in terms of the properties of the enzyme, which implies a role for induced fit in the substrate specificity of ADC. Fersht (*38*) argued that induced fit decreases k_{cat}/K_m by the same amount for any of a series of alternative substrates when a given chemical or other central step is rate-determining, establishing that such an induced fit mechanism cannot result in substrate specificity. Conditions that enable induced fit to enhance substrate specificity have been described (*39*). One such condition occurs when a substrate is surrounded by an enzyme in the catalytically active state, such as by the closure of an active site flap. This has the effect of increasing the number or strength of enzyme−substrate interactions of only substrates for which the enzyme is specific, which provides free energy that can be used for catalysis. Another condition occurs when an alternative substrate is less capable of accelerating the reaction such that the chemical step is rate-determining for the poor substrate, whereas product release is rate-determining for the good substrate. The results shown in this paper and by others, for the mechanistically related enzyme ODC, suggest a rate-determining product release step for ADC catalyzed decarboxylation of the natural substrate (L-arginine). Alternatively, a conformational change (perhaps the closure of an active site flap as occurs in the alanine racemase mechanism) could result in enhanced substrate binding that is sensitive to the guanidinium group and causes acceleration of the chemical step for the correct substrate. The data described herein do not discriminate between these possibilities. In conclusion, the results demonstrate a role for induced fit in the substrate specificity of ADC.

ACKNOWLEDGMENT

We gratefully acknowledge Dr. Robert Perry (University of Kentucky, Department of Microbiology, Immunology, and Molecular Genetics) for providing *Y. pestis* genomic DNA and for the use of his facilities for PCR. We thank Dr. Meg Phillips and Laurie Jackson for helpful discussions. Finally, we thank the reviewers for the time and effort in providing us significant comments to improve the manuscript.

REFERENCES

1. Tabor, C. W., and Tabor, H. (1985) *Microbiol. Rev. 49*, 81−99.
2. Tabor, C. W., and Tabor, H. (1976) *Annu. Rev. Biochem. 45*, 285−306.
3. Gani, D. (1991) *Philos. Trans. R. Soc. London, Ser. B 332*, 131−139.
4. Dunathan, H. C., and Voet, J. G. (1974) *Proc. Natl. Acad. Sci. U.S.A. 71*, 3888−3891.
5. Kirsch, J. F., Eichele, G., Ford, G. C., Vincent, M. G., Jansonius, J. N., Gehring, H., and Christen, P. (1984) *J. Mol. Biol. 174*, 497−525.
6. Dunathan, H. C. (1971) *Adv. Enzymol. Relat. Areas Mol. Biol. 35*, 79−134.
7. Smith, P. K., Krohn, R. I., Hermanson, G. T., Mallia, A. K., Gartner, F. H., Provenzano, M. D., Fujimoto, E. K., Goeke, N. M., Olson, B. J., and Klenk, D. C. (1985) *Anal. Biochem. 150*, 76−85.
8. Fujii, A., and Cook, E. S. (1975) *J. Med. Chem. 18*, 502−505.
9. Norris, K. A., Atkinson, A. R., Smith, W. G. (1975) *Clin. Chem. 22*, 243−245.
10. Wu, W. H., and Morris, D. R. (1973) *J. Biol. Chem. 248*, 1687−1695.
11. Harris, C. M., Johnson, R. J., and Metzler, D. E. (1974) *Biochim. Biophys. Acta 421*, 181−199.
12. Matsushima, Y., and Martell, A. E. (1967) *J. Am. Chem. Soc. 89*, 1322−1330.
13. Metzler, D. E., and Harris, C. M. (1973) *Biochemistry 12*, 5377−5392.
14. Vazquez, M. A., Munoz, F., Donoso, J., and Garcia Blanco, F. (1991) *Biochem. J. 279*, 759−767.
15. Johnson, G. F., Tu, J. I., Bartlett, M. L., and Graves, D. J. (1970) *J. Biol. Chem. 245*, 5560−5568.
16. Shaltiel, S., and Cortijo, M. (1970) *Biochem. Biophys. Res. Commun. 41*, 594−600.
17. Wu, W. H., and Morris, D. R. (1973) *J. Biol. Chem. 248*, 1696−1699.
18. Shaw, J. P., Petsko, G. A., and Ringe, D. (1997) *Biochemistry 36*, 1329−1342.
19. Stamper, G. F., Morollo, A. A., Ringe, D., and Stamper, C. G. (1998) *Biochemistry 37*, 10438−10445.
20. Ray, S. S., Bonanno, J. B., Rajashankar, K. R., Pinho, M. G., He, G., De Lencastre, H., Tomasz, A., and Burley, S. K. (2002) *Structure 10*, 1499−1508.
21. Gokulan, K., Rupp, B., Pavelka, M. S., Jr., Jacobs, W. R., Jr., and Sacchettini, J. C. (2003) *J. Biol. Chem. 278*, 18588−18596.
22. Jackson, L. K., Brooks, H. B., Osterman, A. L., Goldsmith, E. J., and Phillips, M. A. (2000) *Biochemistry 39*, 11247−11257.
23. Grishin, N. V., Osterman, A. L., Brooks, H. B., Phillips, M. A., and Goldsmith, E. J. (1999) *Biochemistry 38*, 15174−15184.

24. Kern, A. D., Oliveira, M. A., Coffino, P., and Hackert, M. L. (1999) *Structure Fold Des. 7*, 567−581.
25. Grishin, N. V., Phillips, M. A., and Goldsmith, E. J. (1995) *Protein Sci. 4*, 1291−1304.
26. Mehta, P. K., and Christen, P. (2000) *Adv. Enzymol. Relat. Areas Mol. Biol. 74*, 129−184.
27. Christen, P., and Mehta, P. K. (2001) *Chem. Rec. 1*, 436−447.
28. Sandmeier, E., Hale, T. I., and Christen, P. (1994) *Eur. J. Biochem. 221*, 997−1002.
29. Jackson, L. K., Goldsmith, E. J., and Phillips, M. A. (2003) *J. Biol. Chem. 278*, 22037−22043.
30. Babbitt, P. C., Mrachko, G. T., Hasson, M. S., Huisman, G. W., Kolter, R., Ringe, D., Petsko, G. A., Kenyon, G. L., and Gerlt, J. A. (1995) *Science 267*, 1159−1161.
31. Babbitt, P. C., Hasson, M. S., Wedekind, J. E., Palmer, D. R., Barrett, W. C., Reed, G. H., Rayment, I., Ringe, D., Kenyon, G. L., and Gerlt, J. A. (1996) *Biochemistry 35*, 16489−16501.
32. Nagano, N., Orengo, C. A., and Thornton, J. M. (2002) *J. Mol. Biol. 321*, 741−765.
33. Phillips, M. A., Coffino, P., and Wang, C. C. (1987) *J. Biol. Chem. 262*, 8721−8727.
34. Osterman, A. L., Kinch, L. N., Grishin, N. V., and Phillips, M. A. (1995) *J. Biol. Chem. 270*, 11797−11802.
35. Osterman, A. L., Brooks, H. B., Rizo, J., and Phillips, M. A. (1997) *Biochemistry 36*, 4558−4567.
36. Brooks, H. B., and Phillips, M. A. (1997) *Biochemistry 36*, 15147−15155.
37. Jackson, L. K., Brooks, H. B., Osterman, A. L., Goldsmith, E. J., and Phillips, M. A. (2000) *Biochemistry 39*, 11247−11257.
38. Fersht, A. R. (1974) *Proc. R. Soc. Lond., Ser. B 187*, 397−407.
39. Herschlag, D. (1988) *Bioorg. Chem. 16*, 62−96.

BI0344127